LIFTING-BASED LOW-LOSS IMAGE COMPRESSION TECHNIQUES FOR CUTTING TOOL IMAGES: A COMPETITIVE STUDY BY RECONSTRUCTION PERFORMANCE ANALYSIS

Fabio Henrique Pereira, fabiohp@uninove.br
Sergio Bezerra Barros, sergio.barros@hotmail.com
Elesandro Baptista, elesandro@elesandroab.eng.br
Nivaldo Lemos Coppini, ncoppini@uninove.br
Industrial Engineering Post Graduation Program, Uninove University, Vergueiro street 235, São Paulo - Brasil.

Abstract. *Usually, the use of the Artificial Intelligence techniques for lifetime prediction is made by detecting visible – sometimes very small – degeneration in images of a cutting tool, which is supplied by a typical experiment in the turning process. In order to make visible small changes or degenerations in a cutting tool, this experiment tends to generate high-resolution images. As finding patterns in high-resolution images can be a hard task to all kind of Artificial Intelligence techniques, it is common apply some low-loss image compression techniques before using the images as input in the prediction process. In this work, we accomplished a comparative study between some of the most known wavelet functions in lifting-based low-loss image compression techniques. The wavelet functions of Haar, Daubechies, Biorthogonal, Coiflets and Symlets has been tested and the numerical results related to the quality of compressed images was measured in terms of distortion measures such as reconstruction error, Mean Square Error and Peak Signal-to-Noise Ratio. The objective is to define the best wavelet function for this specific application because it is known that the selection of proper mother wavelet is one of the important parameters of image compression.*

Keywords*: Cutting tool, Image compression, Lifting technique, Wavelet functions*

1. INTRODUCTION

In the last years, the use of Artificial Intelligence techniques as, for example, artificial neural network, to estimate tool's lifetime in metal cutting process has been the aim of many researches (Alajmi *et al.,* 2005; Patra *et al.*, 2007; Chao and Hwang, 1997; Alajmi and Alfares, 2007). Usually, the lifetime is predicted by detecting visible – sometimes very small – degeneration in images of a cutting tool, which is supplied by a typical experiment in the turning process. In order to make visible small changes or degenerations in a cutting tool, this experiment tends to generate high-resolution images. Finding patterns in high-resolution images can be a hard and time consuming task to the most artificial neural network approaches. So, in order to obtain relevant enhancement in patterns recognition performance, before using images as input cases in the neural network training processes, it is common to apply some low-loss image compression techniques.

Wavelet decomposition is recognized as a powerful tool for image analysis and data compression. In fact, many works has shown how to use wavelets transform for creating data compression methods with great potential to compress large-scale, three-dimensional image data files, while keeping the most important information necessary to find patterns in the data. (Grgeć *et al.*, 2000; Lo *et al.*, 2003; O'Rourke and Stevenson 1995; Uhl, 1997). However, despite its good properties the numerical performance of the wavelet transforms can to be improved through the lifting technique. The lifting technique is a method introduced by W. Sweldens (1996), which allows to create an wavelet transform algorithm with smaller memory requirement and a reduced number of floating point operations, if long filters are used, keeping the efficiency of the technique (Sweldens, 1996; Daubechies and Sweldens, 1998).

In this work, we accomplished a comparative study between some of the most known wavelet functions in lifting-based low-loss image compression techniques for a cutting tool image. The families of wavelet function Haar, Daubechies, Biorthogonal, Coiflets and Symlets has been tested and the numerical results related to the quality of compressed images was measured in terms of distortion measures such as reconstruction error, Mean Square Error and Peak Signal-to-Noise Ratio. The objective is to define the best wavelet function for this specific application and, consequently, to provide a useful reference for helping to choose good wavelet compressions systems for applications involving cutting tool images.

2. LIFTING TECHNIQUE

Over the last few years, the mathematical analysis and the community of signal processing have created several algorithms of compactly supported wavelet. In fact, many other areas of science such as engineering, and mathematics have also contributed to the development of the wavelet field (Sarkar *et al.*, 2002). Due to the different origins of wavelets, their properties and construction can be motivated and understood in different ways. Lifting technique is one of these ways and it has some structural advantages in relation to traditional approaches (Jensen and la Cour-Harbo, 2001; Daubechies and Sweldens, 1998).

Daubechies and Sweldens (1998) have shown that every wavelet functions can be decomposed into lifting steps. Therefore, all data compression methods based on wavelet transforms can be implemented with the lifting scheme. The main advantages of this technique over the classical wavelet transform are (Daubechies and Sweldens, 1998):

a) Smaller memory requirement – the calculations can be performed in-place;
b) Efficiency: reduced number of floating point operations;
c) Parallelism –inherently parallel feature;
d) Easier to understand - not introduced using the Fourier transform;
e) Easier to implement
f) The inverse transform is easier to find – it has exactly the same complexity as the forward transform
g) Transforms signals with an arbitrary length (need not be 2^n with $n \in \mathbb{N}$);
h) Transforms signals with a finite length (without extension of the signal).

The basic idea of this technique is to exploit the correlation present in most real life signals to build a sparse approximation. In contrast to traditional approach, which relies heavily on the frequency domain, the lifting scheme derives all constructions in the spatial domain (Sweldens, 1996). This feature allows that the lifting algorithms can easily be generalized to higher dimensions and complex geometric structures.

For a simple introduction of the lifting scheme we considered a finite signal of length 2^j, which is represented here as:

$$\mathrm{s}^j = \{s_1^j, s_2^j, s_3^j, \ldots, s_{2^j}^j\} \tag{1}$$

The lifting scheme assumes that the numbers $s_i^j, i = 1, \ldots, 2^j$, are not randomly distributed, but contain some correlation between the sample and its neighbors. Then an odd sample s_{2k+1}^j can use the average of its two even neighbors for its prediction. The detail d_k^{j-1} is defined as the difference between the odd sample and its computed prediction (Jensen and la Cour-Harbo, 2001), as expressed by:

$$d_k^{j-1} = s_{2k+1}^j - (s_{2k}^j + s_{2k+2}^j)/2 \tag{2}$$

Therefore, if the sample and its neighbors have almost the same value, then the difference is of course small, and the prediction is good.

To preserve the average value of the original signal the values of the difference are redistributed to the computed averages issued from the prediction phase. This operation is called update and is defined by (3).

$$s_k^{j-1} = s_{2k}^j + (d_{k-1}^{j-1} + d_k^{j-1})/4. \tag{3}$$

This prediction and update steps are of order two. In this case, the prediction will be exact, if the original signal is linear and the update will preserve the average and the first moment. This idea is illustrated in Fig. 1.

The procedure defined by (2) and (3) is only one example that can be used for constructing wavelet transforms and it is part of a large family of so-called biorthogonal wavelet CDF(2,2) transforms.

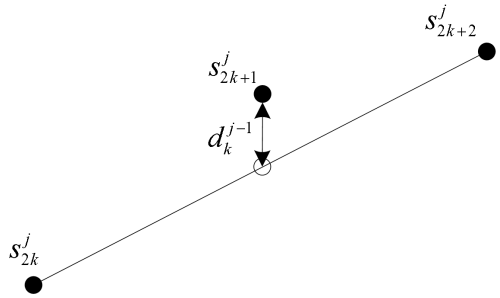

Figure 1. Prediction is correct for a linear signal and the correction is the difference between the real middle sample value and its computed prediction.

As another example of CDF transforms, which have been taken from (Cohen *et al.*, 1992), the detail d_k^{j-1} defined in the expression (2) above can be defined again as

$$d_k^{j-1} = s_{2k+1}^j - \left(9s_k^{j-1} + 3s_{k+1}^{j-1}\right)/8 \tag{4}$$

in which,

$$s_k^{j-1} = s_{2k}^j - \frac{1}{3}s_{2k-1}^j \tag{5}$$

In all these examples of wavelet transforms each pair of prediction and update step is inverted separately, as illustrated in Fig. 3. It is known in the literature that the generalization of this procedure is crucial for application

purposes (Uyterhoeven, *et al.*, 1997). In this generalization a prediction step is followed by an update step and by another prediction and update steps. In this approach the detail d_k^{j-1} can be defined as (6)

$$d_k^{j-1} = \frac{\sqrt{3}+1}{\sqrt{2}} \tilde{d}_k^{j-1}, \tag{6}$$

in which,

$$\tilde{d}_k^{j-1} = s_{2k+1}^j - \frac{1}{4}\sqrt{3}s_k^{j-1} - \frac{1}{4}(\sqrt{3}-2)s_{k-1}^{j-1} \tag{7}$$

and

$$s_k^{j-1} = s_{2k}^j + \sqrt{3}s_{2k+1}^j \tag{8}$$

The operations (6)-(8) are part of one step in the discrete wavelet transform based on Daubechies 4 filters. There are many other examples to build wavelet transforms and some of them can be found in (Uyterhoeven, *et al.*, 1997). Overall, the direct lifting transform can be defined as

$$\begin{aligned} \mathrm{d}_{j-1} &= odd_{j-1} - P(even_{j-1}) \\ \mathrm{s}_{j-1} &= even_{j-1} + U(\mathrm{d}_{j-1}) \end{aligned} \tag{9}$$

where P and U are, respectively, the prediction and update step and the entries s_j are sorted into even and odd entries (of course, in effective implementations the entries are not separated).

The prediction and the update lifting steps are shown in Fig. 2 and the direct and inverse lifting steps in Fig. 3. As can be observed from Fig. 3, the inverse transform is easily found by flipping the order of the operations and inverting its signs. This is an important structural advantage of lifting (Sweldens, 1996).

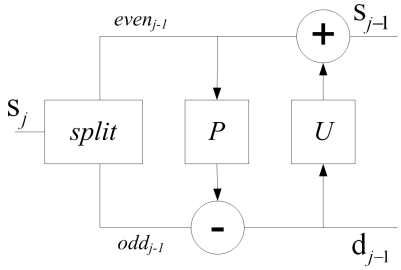

Figure 2. Block diagram of prediction and update lifting steps

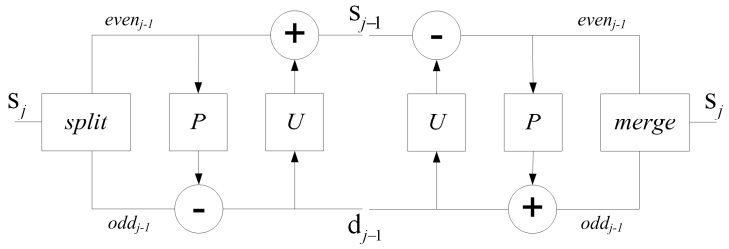

Figure 3. Direct (left side) and inverse (right side) lifting steps

2.1. Lifting-based low-loss image compression techniques

In two-dimensional case the one-dimensional lifting process defined, for example, by the equations (6)-(8), are applied in the rows and columns of the matrix. In this case, the lifting transform generates a matrix formed by four types of coefficients: the approximation coefficients (A), the horizontal (H), the vertical (V), and the diagonal (D) details coefficients. These coefficients are called image sub-bands. The approximation coefficients keep the most important information of the matrix, whereas the details coefficients possess very small values, close to zero. Then, it is possible to choose a value of threshold and set to zero all the details coefficients that are below that value. As result, it is formed a low-loss version of the original image after accomplishing the inverse lifting transform. This decomposition process is part of a multiresolution approach and can be continued using the output approximation coefficients in the current level as an input signal in the next level.

To illustrate the lifting process an example of a single-level lifting decomposition, for a simple synthetic image, is presented in Fig. 4. In this Figure, the upper left plot shows the original image, which is based on a 128×128 matrix where the entries with value 1 correspond to black pixels and all others entries have value zero. The coefficients obtained from a lifting transform with a Daubechies 2 wavelet are shown in upper right plot. The bottom left plot shows the inverse transform for each coefficient. In this case a component of the composition is selected, the other three components are replaced by zeroes and the lifting inverse transform is applied. The rebuilt image is presented in bottom right plot.

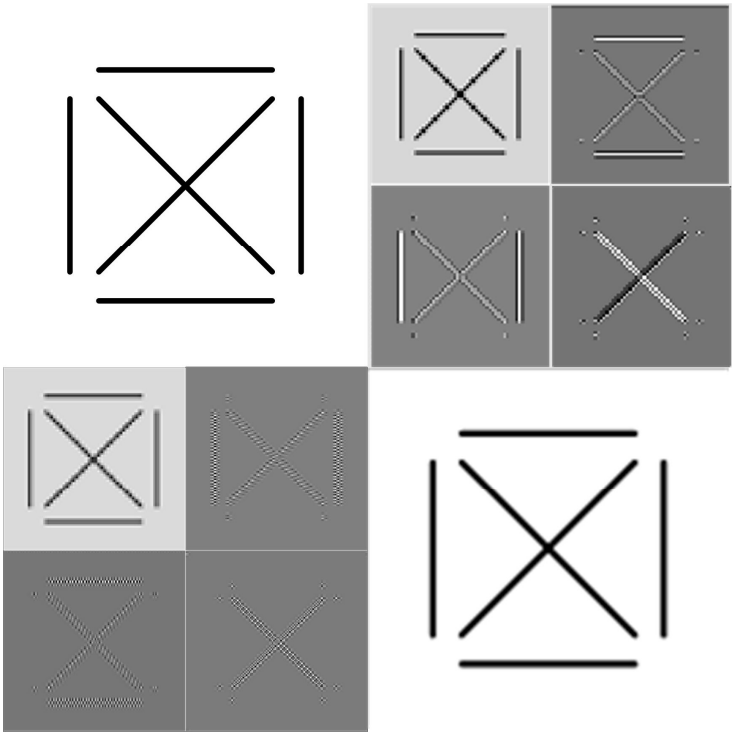

Figure 4. Single-level lifting transform for a simple synthetic image.

This example clearly shows the averaging, and the emphasis of vertical, horizontal, and diagonal lines, respectively, in the four components of the output image. In this example, no value of threshold has been used and the inverse lifting transform rebuilt the original image without any loss of information. In order to be able to see the details, the grey scale has been adjusted in each of blocks of the transform, such that the largest value in block corresponds to black and the smallest value in a block to white.

3. Experimental Results

This work accomplish a comparative study between some of the most known families of wavelet function in lifting-based low-loss image compression techniques for a cutting tool image. The wavelets of Daubechies, Biorthogonal, Coiflets and Symlets have been tested and the numerical results related to the quality of compression are presented. The tests were accomplished using the high-performance language for technical computing MATLAB®.

The low-loss image compression quality provided by these techniques was expressed in terms of the compression factor (ρ), the Mean Square Error (MSE) in approximating the original image U by its compressed version U' and the Peak Signal-to-Noise Rate (PSNR) provided by the image compression process i.e., the ratio between the maximum possible component of U and the power of MSE (noise) that affects the fidelity of the approximation, as defined in Eq. (10)-(12).

$$\rho = \frac{\text{The total storage unit need to represet } U'}{\text{The total storage unit need to represet } U}, \tag{10}$$

$$MSE = \sum_{i=0}^{L-1} (u'_i - u_i)^T (u'_i - u_i) \tag{11}$$

and the PSNR

$$PSNR = 10\log\left(\frac{(\max comp\{U\})^2}{MSE}\right) \tag{12}$$

We also presented the Rate vs. Peak Signal-to-Noise Ratio curves for the different wavelet functions tested in this work, which are shown in Tab. 1. The Rate is defined as the average number of bits per pixel in a compressed image (Lo *et al.*, 2003).

Table 1. Wavelet functions used in the numerical tests

Families of wavelet functions		
Daubechies	*Coiflets and Symlets*	*Biorthogonal*
db1	coif1	bior1.1
db2	coif2	bior1.3
db3	sym2	bior2.2
db4	sym3	bior2.4
db5	sym4	bior3.1
db6	sym5	bior3.3
db8	sym6	bior4.4

The original cutting tool image used in the tests is presented in Fig. 5. Details related to the memory request for this image are shown in the second row of the Tab. 2.
Three values of compression rate were previously selected and the resulting compressed images were analyzed by comparing distortion measures mentioned above. These experimental results are shown in Tab. 2-4. Table 2 presents the results for a compression rate of, approximately, 0.190. The compression rate is defined as *1 - compression factor*, which is calculated as (10).

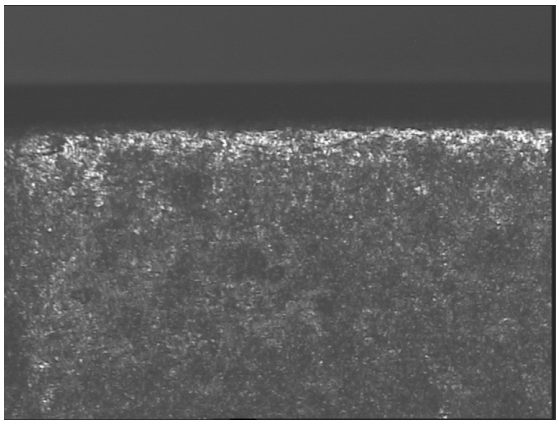

Figure 5. The original 768x576 pixel cutting tool image (Tagged Image File Format - TIFF)

Tables 3 and 4 present similar results with compression rates of 0.405 and 0.919, respectively. However, in this case only the best cases (higher PSNR) are presented. For compression rate of 0.919, only three wavelet functions produced acceptable results (Table 4). Is important to note that the Lifting technique with Biorthogonal wavelet *bior1.1* and with the Daubechies wavelet *db1* are numerically the same. The same is true for Daubechies wavelet *db2* and Symlet wavelet *sym2*.

The corresponding compresses images for some of these cases are illustrated in Fig. 6.

Table 2. Results for different wavelet functions in Lifting-based low-loss image compression techniques (compression rate of approximately 0.190)

	Image compression technique	Memory request	Compression factor (ρ)	Compression Rate (1 - ρ)	PSNR (*decibels*-dB)
	Original Image	430276	-	-	-
Wavelets of Daubechies	Lifting db1	348523	0.810	0.190	48.22
	Lifting db2	350503	0.814	0.185	43.94
	Lifting db3	352740	0.819	0.180	44.19
	Lifting db4	350890	0.815	0.184	43.90
	Lifting db5	349169	0.811	0.188	42.84
	Lifting db6	349956	0.813	0.186	37.80
	Lifting db8	348544	0.810	0.190	30.99
Wavelets of Coiflets and Symlets	Lifting coif1	347706	0.808	0.191	12.33
	Lifting coif2	349599	0.812	0.187	28.11
	Lifting sym2	350503	0.814	0.185	43.94
	Lifting sym3	348781	0.810	0.189	44.23
	Lifting sym4	352740	0.819	0.180	45.01
	Lifting sym5	348308	0.809	0.190	44.66
	Lifting sym6	348480	0.809	0.190	17.64
Biorthogonal wavelets	Lifting bior1.1	348523	0.810	0.190	48.22
	Lifting bior1.3	349298	0.811	0.188	45.64
	Lifting bior2.2	350201	0.813	0.186	43.37
	Lifting bior2.4	350072	0.813	0.186	43.72
	Lifting bior3.1	348566	0.810	0.189	26.58
	Lifting bior3.3	348910	0.810	0.189	38.45
	Lifting bior4.4	350847	0.815	0.184	43.67

Table 3. Results of Lifting-based low-loss image compression techniques for compression rate of approximately 0. 4050

Image compression technique	Memory request	Compression factor (ρ)	Compression Rate (1 - ρ)	PSNR (*decibels*-dB)
Original Image	430276	-	-	-
Lifting db1	256875	0.597	0.403	38.42
Lifting db2	256229	0.595	0.404	27.97
Lifting sym2	256229	0.595	0.404	27.97
Lifting sym5	256014	0.595	0.405	27.62
Lifting bior1.1	256875	0.597	0.403	38.42
Lifting bior1.3	256100	0.595	0.405	35.83

Table 4. Results of Lifting-based low-loss image compression techniques for compression rate of approximately 0.919

Image compression technique	Memory request	Compression factor (ρ)	Compression Rate (1 - ρ)	PSNR (*decibels*-dB)
Original Image	430276	-	-	-
Lifting db1	34852	0.081	0.919	25.87
Lifting bior1.1	34852	0.081	0.919	25.87
Lifting bior1.3	36573	0.085	0.915	25.45

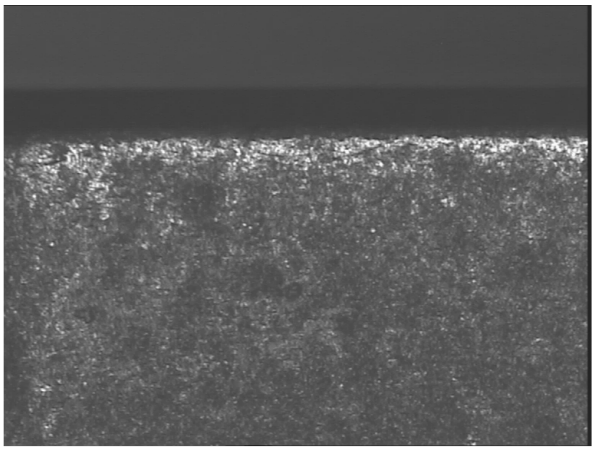

Lifting *db1* (compression rate of 0.190)

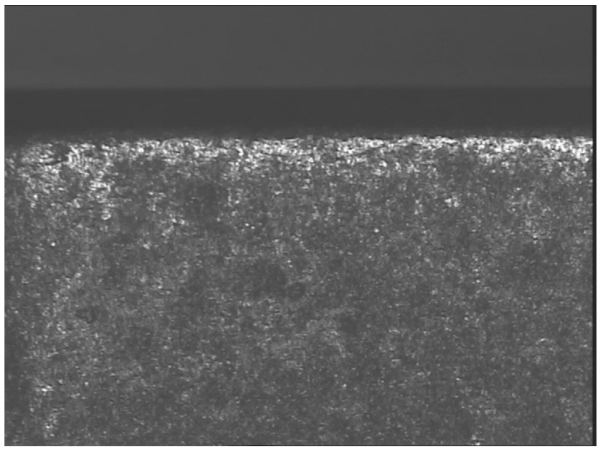

Lifting *bior1.3* (compression rate of 0.188)

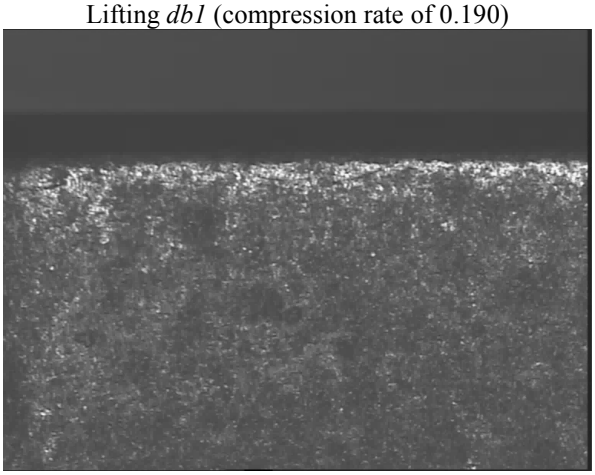

Lifting *db1* (compression rate of 0.403)

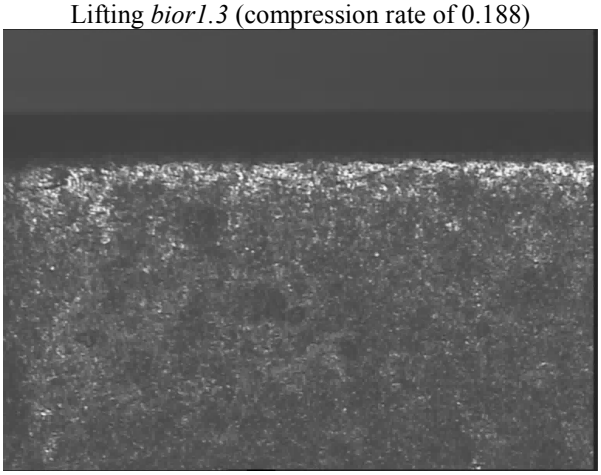

Lifting *bior1.3* (compression rate of 0.405)

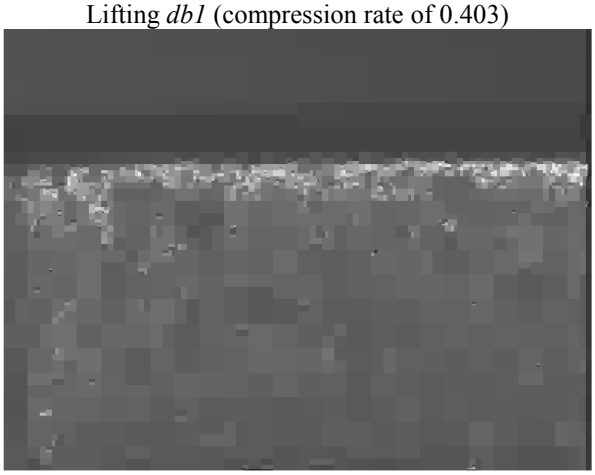

Lifting *bd1* (compression rate of 0.919)

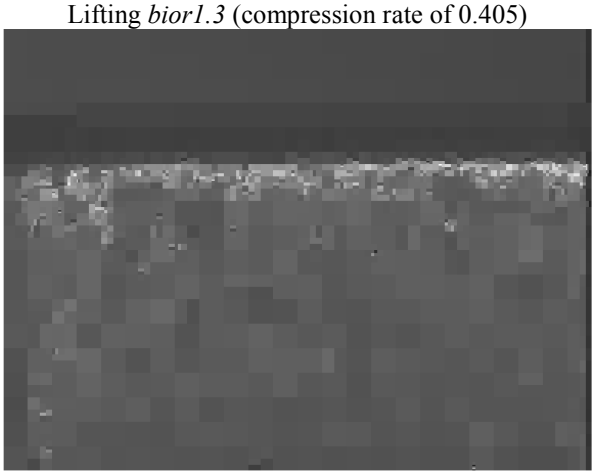

Lifting *bior1.3* (compression rate of 915)

Figure 6. Compressed image corresponding to the two best cases (higher PSNR) from Tables 2, 3 and 4

Finally, the Rate vs. Peak Signal-to-Noise Ratio curves for all wavelet functions tested are presented in Fig. 7. Figure 7 presents the results separate in sets of wavelet functions. Figures 7a, 7b and 7c show the curves for Daubechies, Coiflets and Symlets, and Biorthogonal wavelets, respectively. The Rate vs. Peak Signal-to-Noise Ratio curves for the six best cases are presented in Fig. 7d.

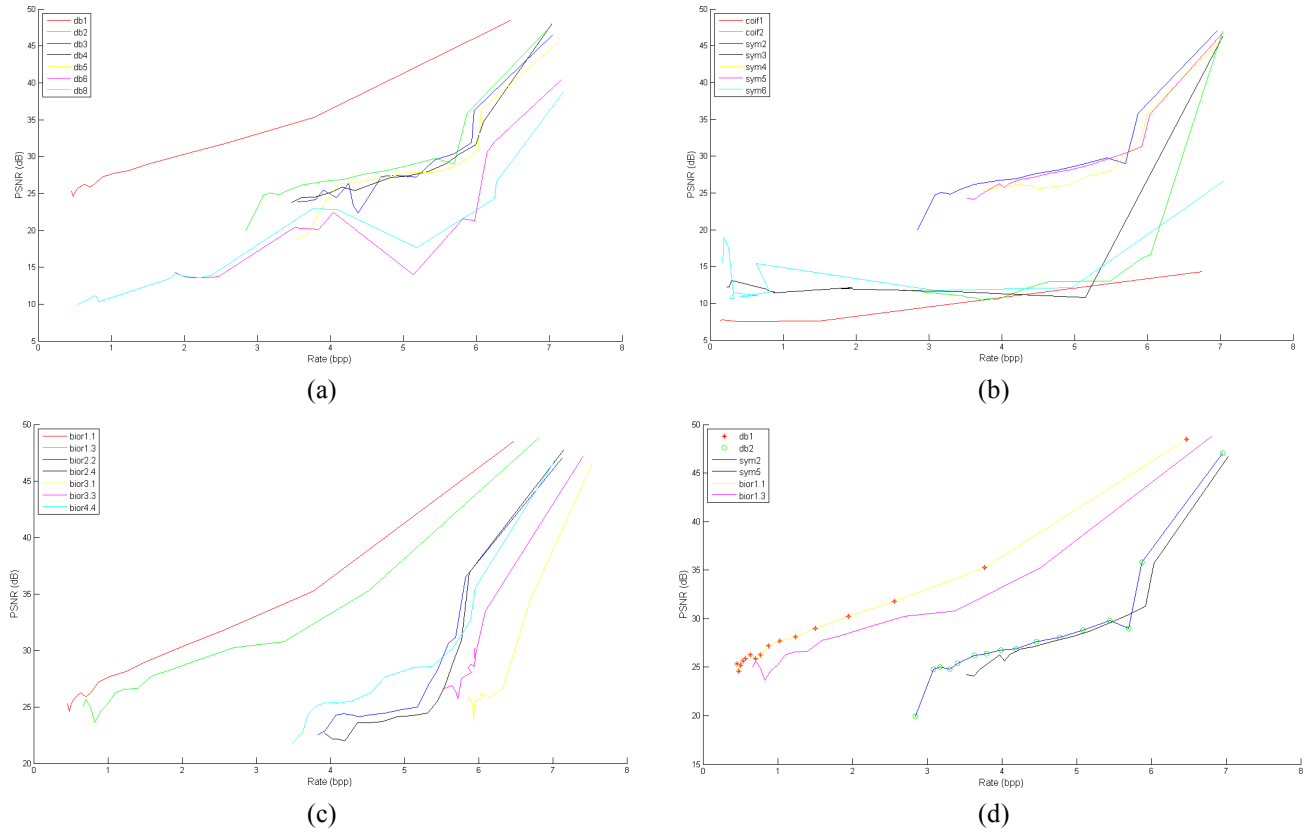

Figure 7. Rate vs. Peak Signal-to-Noise Ratio curves for all wavelet functions tested: (a) Daubechies wavelets, (b) Coiflets and Symlets wavelets, (c) Biorthogonal wavelets and (d) the six best cases in (a), (b) and (c).

4. CONCLUSIONS AND COMENTS

In this paper a comparative study between some of the most known families of wavelet function in lifting-based low-loss image compression techniques for a cutting tool image has been presented. The objective is to define the best wavelet function for this specific application because it is known that the selection of proper mother wavelet is one of the important parameters of image compression. The wavelets of Daubechies, Biorthogonal, Coiflets and Symlets have been tested and the numerical results related to the quality of compression were presented. The results demonstrate that, in general, the *db1* (or *bior1.1*) and *bior1.3* perform significantly better for all the compression rates. In fact, if an aggressive thresholding is applied for get high values of compression rate the wavelets of *db1* (or *bior1.1*) and *bior1.3* are the only choices for the tested case, as shown the results in Tables 3 and 4. However, if a low compression rate is sufficient it is possible to use the Daubechies wavelets *db2*, *db3*, *db4* and *db5* as well as the Symlet wavelets (*sym2*, *sym3*, *sym4* and *sym5*) or the Biorthogonal wavelets (*bior2.2*, *bior2.4* and *bior4.4*). On the other hand, the Coiflets wavelets and the wavelets *db6*, *db8*, *sym6*, *bior3.1* and *bior3.3* are not the best choice for this application. These results are summarized in Fig. 7 which presents the Rate vs. Peak Signal-to-Noise Ratio curves for all wavelet functions used in this work.

5. REFERENCES

Alajmi, M. S., Alfares. F., 2007, "Prediction of Cutting Forces in Turning Process using De-Neural Networks**",** Proceedings of the 25th IASTED International Multi-Conference: Artificial Intelligence and Applications**,** Innsbruck, Austria, pp. 41-46.

Alajmi, M. S., Oraby, S. E., and Esat, I. I., 2005, "Neural Network Models on the Prediction of Tool Wear in Turning Process: A Comparison Study", presented at IASTED Conference on Artificial Intelligence and Applications, AIA 2005, Innsbruck, Austria.

Chao, P. Y. and Hwang, Y. D., 1997, "An improved neural network model for the prediction of cutting tool life", Journal of Intelligent Manufacturing, Vol. 8, No. 2, pp. 107-115.

Cohen, A., Daubechies, I. and Feauveau, J.-C., 1992, "Biorthogonal bases of compactly supported wavelets", Comm. Pure Appl. Math., Vol. 45, No. 5, pp. 485-560.

Daubechies, I and Sweldens, W., 1998, "Factoring Wavelet Transforms into Lifting Steps", J. Fourier Anal. Appl., 1998, Vol. 4, No 3, pp. 245-267.

Grgeć, S., Grgeć, M. and Zovko-Cihlar, B, 2000, "Optimal Decomposition for wavelet Image Compression", in First International Workshop on Image and Signal Processing and Analysis, Pula, Croatia, pp. 14-15.

Jensen, A. and la Cour-Harbo, A., 2001, "The Discrete Wavelet Transform, Ripples in Mathematics", Springer, Berlin.

Lo, S.-C.B.; Huai Li; Freedman, M.T., 2003, "Optimization of wavelet decomposition for image compression and feature preservation", IEEE Transactions on Medical Imaging, Vol. 22, No. 9, pp. 1141-1151.

O'Rourke, T. P. and Stevenson, R. L., 1995, "Human Visual System Based Wavelet Decomposition for Image Compression", Jounal of Visual Comm. and Image Repressentation, Vol. 6, pp. 109-121.

Patra, K., Pal, S. K., and Bhattacharyya, K., 2007, "Artificial Neural Network Based Prediction of Drill Flank Wear From Motor Current Signals", *Applied Soft Computing Journal*, Vol. 7, pp. 929-935.

Sarkar, T. K., Magdalena, S. P. and Michael, C. W., 2002, "*Wavelet Applications in Engineering Electromagnetics"*, Artech House, Boston.

Sweldens, W., 1996, "The lifting scheme: A custom-design construction of biorthogonal wavelets". Appl. Comput. Harmon. Analysis., Vol. 3, No. 2, pp. 186-200.

Sweldens W. and Schröder, P., 1996, "Building your own wavelets at home". In Wavelets in Computer Graphics, ACM SIGGRAPH Course Notes.

Uhl, A., 1997, "Generalized Wavelet Decompositions in Image Compression: Arbitrary Subbands and Parallel Algorithms", Optical Engineering, Vol. 36, No. 5, pp. 1480-1487.

Uyterhoeven, G., Roose, D. and Bultheel, A., 1997, "Wavelets transform using the lifting scheme", Report ITA-Wavelets-WP1.1 (Revised version), Departament of Computer Science, K. U. Leuven, Heverlee, Belgium.

6. RESPONSIBILITY NOTICE

The authors are the only responsible for the printed material included in this paper.